Tomographic Imaging of a Snowpack

RICHARD FORTIN[1] AND RICHARD FORTIER[2]

ABSTRACT

Measuring the physical properties of snow cover is a challenging task that involves destructive sampling. Ground penetrating radar (GPR) provides a mean to probe a snowpack with limited intrusion. The potential of GPR for imaging a cross section of a snow cover was examined while evaluating the decimetric scale variability of a snow cover. Tomographic imaging of a snow pack was performed with a bistatic GPR operating at 900 MHz. Data acquisition was performed on a 72 cm high seasonal snowpack on a cold day (-10°C). A 150 cm thick snow wall was delineated by two parallel trenches. Shot points and receiving points were located at equally spaced intervals along the height of the snow wall's faces. The traveltime of GPR pulses in the snow wall from the transmitting to the receiving antenna was measured for each shot point to every receiving points. In a first step, the subset of horizontal transmission was compared with a vertical profile of snow density and permittivity. Results show that traveltime data are sensitive to small changes in snow density. The next step consisted in performing a tomographic inversion of the data set with an algorithm devised to be biased toward horizontal stratification. This design limited the creation of artefacts in the final 2-D image without preventing the resolution of horizontal variabilities. The resulting tomographic image shows that a more complete image of the snowpack is obtained in comparison with the snow pit observations or with the vertical profile of the permittivity. The image also shows that thermal interactions at the wall's faces significantly affect the snow physical properties. Overall, the tomographic imaging of a snowpack gave conclusive results. Therefore, this methodology could be extended to monitor snow cover evolution, characterize small-scale variability and detect features like melt pathways or ice columns.

Key words: Snow, ground penetrating radar, tomography, permittivity

INTRODUCTION

A fundamental feature of seasonal snow cover is its spatial variability at all scale of observation (Marsh, 1999). At the large scale of an entire drainage basin, the variability is important and, it is possible to have some locations exhibiting a snow cover of a few meter thick, while other locations are almost free of any snow cover. This is a realization of the variability of the landscape and of the meteorological conditions. For example, topography, vegetative cover and wind are parameters that influence the drifting of snow and therefore contribute to the accumulation or depletion of snow. Also, air temperature variability results in deposition and accumulation of snow at given locations, or rain and melting at others. At smaller scale, variability in the snow cover can still be significant even though variations of the ground surface and of the local meteorology are less important. At the scale of a few times the thickness of a snowpack,

[1] Département de Génie Civil, Université Laval, Québec, Canada, G1K 7P4, telephone: 613-990-6118
Fax: 613-954-1235, E-mail: richard.fortin@nrc.ca
[2] Département de Géologie et de Génie Géologique, Québec, Canada, G1K 7P4, telephone: 418-656-2746
Fax: 418-656-7339, E-mail: rifortie@ggl.ulaval.ca

variability can be described at two level. The stratigraphy of a snowpack in layers of new snow, rounded grains and depth hoar, with the eventual occurences of ice layers, define in the first hand, the vertical variations, which represent the predominant variability in a snowpack at this scale of observation. On the other hand, second order variations in the thickness and density of snow layers, discontinuity in the ice layers, melt pathways and ice columns are typical horizontal variations.

Physical processes in the snowpack depend on the snow physical properties. At some moment, the structure of a snowpack and its variability are the result of the snowpack evolution, but they also constitute parameters for further changes. In hydrologic studies, there is an important interest given to snow cover melting and the ensuing runoff process. Since snow water equivalent is determined by the snow density, better estimates of the runoff will be obtained if the snow cover variability is quantified. It is therefore important to characterize the variability of a snow cover in order to understand these processes.

Subsurface radar, or ground penetrating radar (GPR), probing provides a promising method to characterize the structure of a snow cover at an intermediate scale of observation between a complete description obtained from a snow pit and an image of a snow covered surface obtained by a spaceborne remote sensing instrument. Moreover, subsurface radar can be used to estimate the depth (Holmgren et al., 1998) or the water equivalent (Vickers and Rose, 1973; Ellerbruch and Boyne, 1980) of a snow cover, to characterize the percolation of melt water (Gubler and Hiller, 1984; Albert et al., 1999), and to locate weak layers in a snowpack (Gubler and Weilenmann, 1986; Niessen et al., 1994). The potential of GPR for imaging the cross section of a snowpack by tomographic inversion will be evaluated here while characterizing the decimetric scale variability of a seasonal snowpack. Tomography is an imaging technique that provides a two dimensional (2-D) image of the plane section of an object, and appears to be an appropriate methodology to evaluate snow cover spatial variability.

DATA ACQUISITION AND ANALYSIS

The velocity v of an electromagnetic (EM) pulse propagating in a given low loss material like dry snow is a function the dielectric permittivity ε of the material. The average velocity of an EM pulse can be readily evaluated from a measurement of the traveltime t of the pulse if the distance d travelled by the pulse in the material is known. Since the permittivity of snow is related to its physical properties, including density, wetness and texture (Ambach and Denoth, 1972, Tiuri et al., 1984, Mätzler, 1996), it provides an indirect measurement of the snow properties. In the first order, given that the permittivity ε of dry snow depends only on the density ρ of the snow according to $\varepsilon = 2\cdot\rho + 1$ (Tiuri et al., 1984), these quantities are related as follows:

$$\rho = \frac{1}{2}(\varepsilon - 1) = \frac{1}{2}\left(\frac{c^2}{v^2} - 1\right) = \frac{1}{2}\left(\frac{c^2 t^2}{d^2} - 1\right), \qquad (1)$$

where c=30 cm/ns is the velocity of light (1 ns = $1\cdot10^{-9}$s). Table 1 give numerical equivalences for this relation in a range of values relevant to seasonnal dry snow.

A bistatic GPR is a radar system that consists of separate transmitting and receiving antennas. It transmits an EM pulse from the transmitting antenna and records the EM field that reaches the receiving antenna. If the antennas are located along the opposite faces of a snow wall excavated in the snow cover the transmitted pulse travels through the snow wall before reaching the receiving antenna. On the resulting radar scan, the average velocity of the pulse in the snow can be evaluated by measuring the traveltime of the pulse.

Data acquisition was performed on march 8, 1998 in an open field near Forêt Montmorency north of Québec city, while the air temperature was -10^{o}C and the snowpack height was 72 cm on average. The snow cover was typical of late winter before the beginning of the melting season. Snow layers consisted mostly of rounded snow grains with few exceptions of faceted crystals. Ice layers were also present. The profiles of density and temperature obtained in the snowpack are presented in Figure 1.

Table 1. The EM velocity and the permittivity of dry snow for a given snow density.

density of snow ρ (g/cm^3)	EM velocity v (cm/ns)	permittivity ε
0.10	27.39	1.20
0.15	26.31	1.30
0.20	25.35	1.40
0.25	24.49	1.50
0.30	23.72	1.60
0.35	23.01	1.70
0.40	22.36	1.80
0.45	21.76	1.90
0.50	21.21	2.00

A 150 cm thick snow wall was excavated in the snow cover by digging two parrallel trenches. In one trench, 12 shot points were located at 5 cm interval along the vertical of the snow wall face from a height of 10 cm up to 65 cm. Receiving point were located at equivalent positions on the opposite face of the snow wall. Every possible raypath is then contained in the same vertical plane section. Shot and receiving points indicate the locations of the transmitting and receiving antennas during data acquisition.

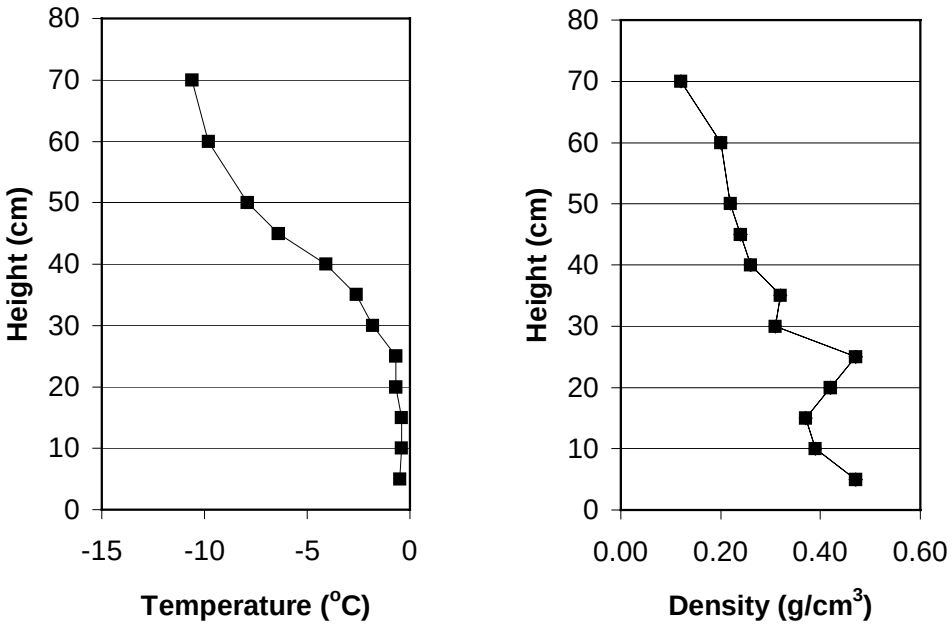

a) b)

Figure 1. Profile of a) temperature and b) density of the snowpack at the investigated site.

A commercially available GPR system (Sensors and Software's PulseEKKO 1000) was used for data acquisition with a pair of antenna of a nominal frequency of 900 MHz. During pulse transmission, the antennas were put in contact with the snow wall faces to maximize the EM energy transmission toward the snow wall. It caused the center frequency of the pulse to decrease

to about 750 MHz. Two data sets were assembled and analyzed, according to the two following situations:

Horizontal transmission and Vertical profiling

A pulse was transmitted in the snow wall for shot and receiving points at the same height along the snow wall's faces (Figure 2a). The traveltime measured on the radar scan is used to evaluate the average velocity along the horizontal raypath connecting the shot to the receiving point. Moreover, using relation (1) with d =150 cm, a vertical profile of the permittivity in the snowpack is obtained. A dielectric profile was also obtained in the trench with a flat capacitance sensor (CS) (Denoth, 1988). This measuring device operates at a frequency of 20 MHz and samples a volume of 14.0 × 12.5 × 3.0 cm. The objective pursued in this part of the data acquisition is to evaluate the dielectric resolution of GPR measurement.

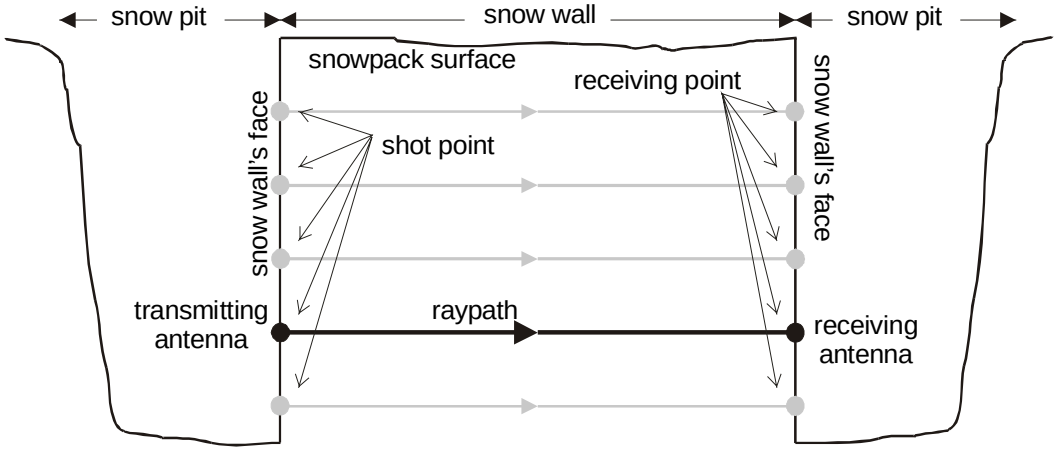

a)

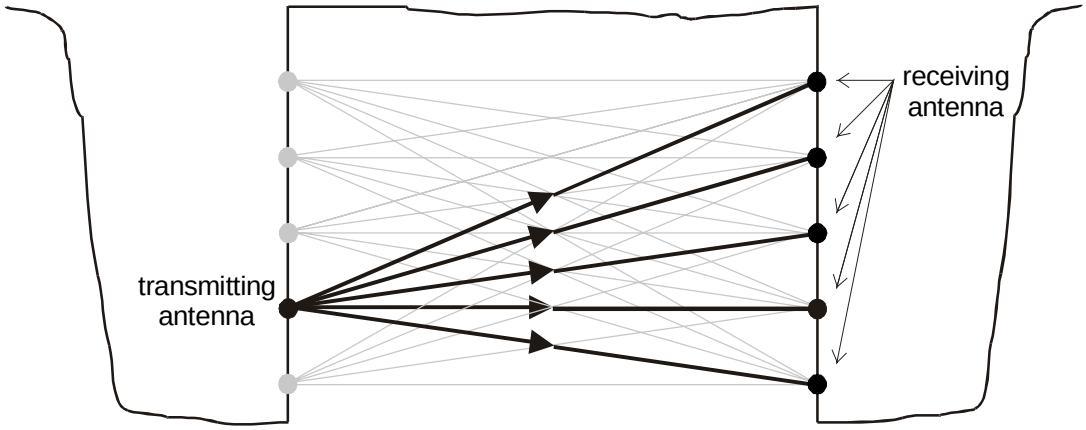

b)

Figure 2. A snow wall excavated in the snow cover where GPR pulse transmission can be performed. The GPR antenna are located along opposite side of the snow wall so that the EM pulse travel through the wall before reaching the receiving antenna.
A) Horizontal transmission (see text) and B) Projections (see text).

Projections and Tomography

While the transmitting antenna was located at a given shot point, a pulse was transmitted for every receiving point (Figure 1b). This fan beam coverage of the snow wall section defines a *projection*. A projection was obtained for every shot point and the resulting data set consists of 144 traveltime data that provide a near complete coverage of the snow wall section.

Traveltime tomography is an inversion technique from which the velocity distribution of the plane section of an object can be reconstructed from traveltime data in projections. The plane section is divided in a grid of rectangular cells and an initial velocity value is assigned to each cell. Synthetic traveltimes are evaluated for this model plane. A tomography algorithm optimizes iteratively the response of the model, the synthetic traveltime, in regard of the measured traveltime, by slightly changing at each step the model plane parameters, specifically here the velocities assigned to the cells. The final result is a tomographic image of the plane section of the object.

For the data set described here, the snow wall model consisted of 60 cells, 5 along the horizontal and 12 along the vertical, and raypaths were approximated by straight lines connecting the shot to the receiving point. The grid and cell's dimensions define the final resolution of the tomographic image. The ART algorithm (Herman et al., 1973; Dines and Lytle, 1979; McMechan, 1983) was used for tomographic inversion. However, the original ART algorithm was modified to account for snow cover physical context. Since the horizontal layering is the main determinant of snowpack structure at this scale of observation, the algorithm should preferably look for a solution exhibiting such a structure. In order to bias the algorithm toward horizontal solution, a horizontal initial model constructed from the vertical profile obtained before (as described in the preceding subsection) was given to the algorithm, and a limiting range of variation around the initial model parameters was set in the inversion scheme. For example, if the limiting range is set to 2 cm/ns and a given cell is assign initially a value of 25 cm/ns, the final result for this cell will be included in the range from 23 cm/ns to 27 cm/ns. This limiting range was the same for all cells and was tested at 1 cm/ns and 2 cm/ns. These values are not physically restrictive since the range of variations of EM velocity in snow is included between 20 cm/ns and 28 cm/ns. Also, 2 cm/ns and 1 cm/ns translate in numerically wider snow density variations. 1 cm/ns proved to be the best choice, providing solution with less artefacts (Fortin, 2000). This modification to the algorithm succesfully contributed to accelerate the convergence of the algorithm, avoid physically unreasonable solutions, and limit the creation of artefacts in the final image.

RESULTS AND DISCUSSION

Horizontal transmission

The permittivity profile of the snowpack obtained from GPR horizontal transmission is presented in Figure 3a). In b), the permittivity profile obtained with the capacitance sensor is also presented. In a first step of evaluation, the GPR permittivity are compared with the capacitance sensor permittivity in Figure 4, where GPR data are plotted against the corresponding CS data. A regression line was computed and forced to pass through the point (1,1) since both instrument should give the same measure for free space. The GPR permittivity are in agreement with the CS data, and the regression formula $y = mx + b$ shows that the two data sets tend to be equal to each other since m and b respectively approach 1 and 0. In the range of 1 MHz to 1 GHz, many experimental results have demonstrated (Ambach and Denoth, 1972, Tiuri et al., 1984) that there is only a slight dependance of the permittivity of snow and ice with frequency and, for practical purposes the permittivity can be considered to be constant in this range. Therefore the results obtained here are in agreement with the expected behavior of the permittivity of snow.

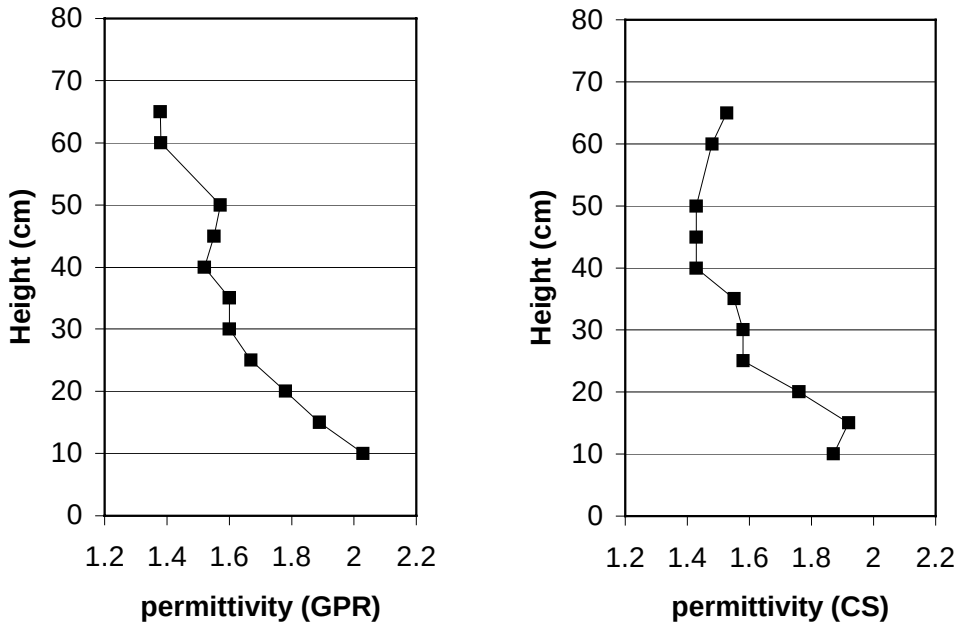

a) b)

Figure 3. Profile of the permittivity in the snowpack obtained from a) GPR and b) capacitance sensor. The presence of an ice layer at 55 cm prevented data acquisition with CS. The GPR data has been removed in a) for the comparison, although this measurement was obtained.

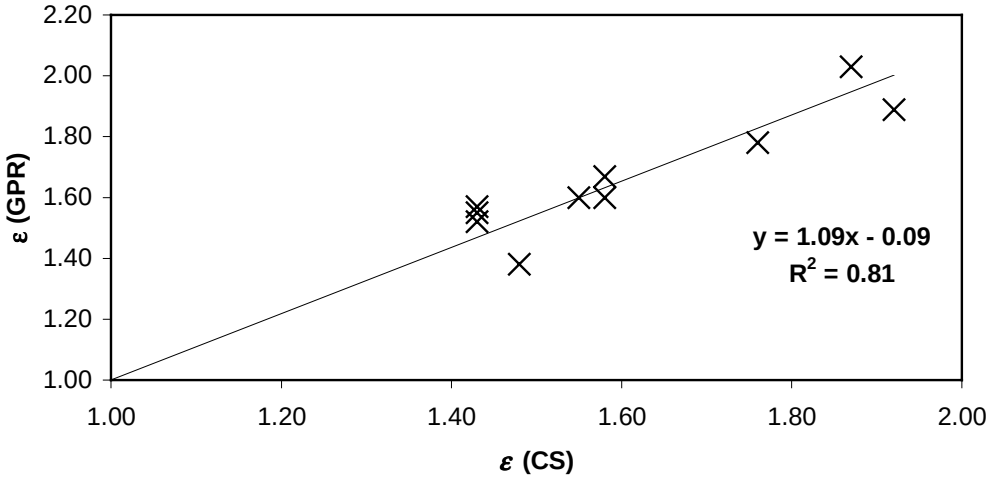

Figure 4. Measurements of the permittivity of snow obtained from GPR in comparison with the corresponding measurements obtained with CS. The regression was forced to contained the point (1,1).

In a second step, GPR permittivities are compared with density measurements in Figure 5, by a linear regression of the data that is forced to contained the point (0,1) since the permittivity of vacuum is 1. The regression formula is in close agreement with other accepted formula found in the litterature, as shown in Table 2.

Table 2. Proposed quantitative relation between density of dry snow and its permittivity.

Formula	Source
$\varepsilon = 2.0 \cdot \rho + 1$	This study
$\varepsilon = 2.2 \cdot \rho + 1$	Ambach and Denoth, 1972
$\varepsilon = 2.0 \cdot \rho + 1$	Tiuri et al, 1984

However, a significant scattering of the data around the regression line is present and results in a relatively low coefficient of determination R^2 (R^2=0.44). It is argumented that this scattering is imputable to the difficulties involved in measuring snow properties. Altough each triplet of data (GPR, CS and density) was obtained at the same height in the snow cover, they were not colocated since CS and density sampling (with a snow cutter) implied destructive operation. Also in each case a different volume of snow was sampled, 100 cm^3, 525 cm^3, and at least 45 000 cm^3 respectively for the snow cutter, CS and GPR, where GPR sampled volume is approximated by the volume included between the antenna. Moreover, density and CS sampling are performed at the snow wall's face where thermal interactions with the ambiant air might occur, while the volume sampled by GPR is much less exposed to thermal interactions at the snow wall's surfaces, and is therefore isolated from artificial processes.

Overall, it is concluded that GPR traveltime measurements are related to snow physical properties. A significant variation of the GPR-derived permittivity is observed for small changes in snow density. However more experimentations are needed to quantify precisely the relation between GPR-derived measurements and snow physical properties. Nevertheless, the results presented here are sufficient to justify the development of a tomographic imaging algorithm.

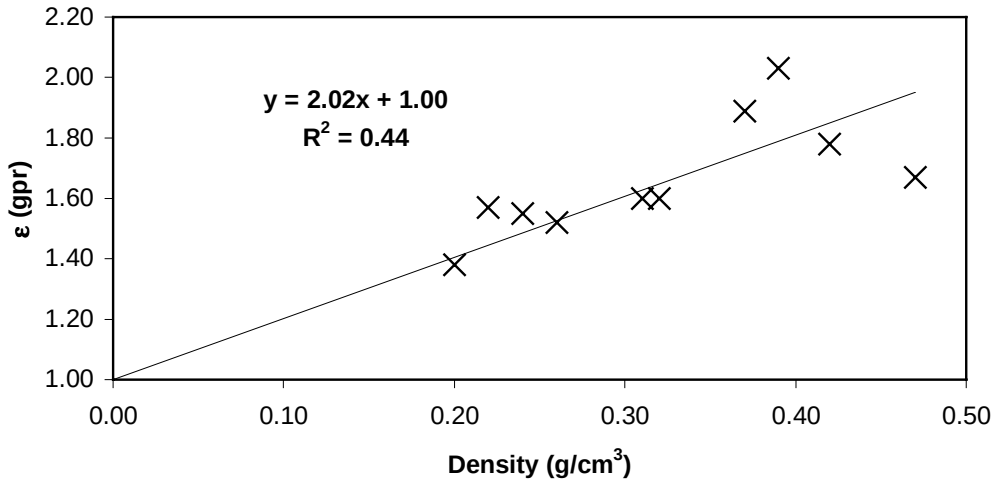

Figure 5. Measurements of the permittivity of snow obtained from GPR in comparison with the density of the snow.

Tomography

The resulting tomographic image of the snowpack using the algorithm described above with a limiting range of 1 cm/ns is presented in Figure 6. The velocity values were translated in density values using the regression formula of figure 5. The main feature of this image is the low density anomaly to the right side of the image that interrrupts the horizontal layering of the left side. This region extends laterally from the snow wall's right face to 80 cm in the snowpack, while its vertical extent is about 40 cm at the snow wall surface, but is narrower as it extends into the subsurface. The average density of this anomaly is. 0.22 $g \cdot cm^{-3}$ (25 cm/ns). It is believed that this

anomaly represents a physical feature of the snow, and is not an artifact created by the algorithm. Numerical simulation that were conducted to test the algorithm (Fortin, 2000) showed that in situation where artifacts creation was promoted by the algorithm, artifacts occurred in the center cells of the grid model or in symmetrical pairs.

However, this anomaly does not seem to result from natural processes in the snowpack, and is probably caused by a transformation of the state of the snow as the trenches were excavated. The snow wall surfaces received a significant and differential input of solar energy. Notably, the right face was exposed to solar irradiation for a longer period of time. Moreover, the drier and colder ambient air came into contact with the snow. A metamorphic process was probably established as the water vapor escaped or crystallized on the snow grains. Similar processes and their influence on radar signature have been observed on the surface of the snow cover (Ellerbruch and Boyne, 1980; Gubler and Hiller, 1984). Changes in temperature and irradiation were invoked then to have contributed to a rapid transformation of the state of the snow, and it is believed that a similar phenomenon occurred here.

CONCLUSION

GPR tomographic imaging of a snowpack is a promising technique for the investigation of snowpack. It provides a 2-D image of a snowpack from which the variability of snow properties can be quantified. The results presented here demonstrate that the traveltime of a GPR pulse is representative of the properties of snow along its raypath, even when considering the finite resolution of the acquisition system and the sources of noise that contaminate the measurements. Altough the tomographic image obtained here presents the effect of an artificial process, it nevertheless demonstrate that internal process can be resolved. To obtain an accurate image of snowpack, efforts should be made to inhibit the interactions of the ambient conditions with the snow wall surfaces by covering the snow wall's faces and by conducting the data acquisition promptly.

Overall, the tomographic imaging of the snowpack gave conclusive results. Therefore, with the possibilities of enhancing the spatial resolution by modifying the data acquisition geometry and adding shot and receiving points, this methodology could be extended to monitor internal processes in snowpack, characterize small-scale variability and detect features like melt pathways and ice columns.

REFERENCES

Albert, M., G. Koh and F. Perron. 1999. Radar investigations of melt pathways in a natural snowpack. *Hydrol. Process.*, 13, 2991-3000.

Ambach, W. and A. Denoth. 1972. Studies on the dielectric properties of snow. *Z. Gletscherk. Glazialgeol.*, 8, 113-123.

Denoth, A. 1988. *The snow surface dielectric device*. operation's manual, University of Innsbruck.

Dines, K. A. and R. J. Lytle. 1979. Computerized geophysical tomography. *Proc. IEEE*, 67(7), 1065-1073.

Ellerbruch, D. A. and H. S. Boyne. 1980. Snow stratigraphy and water equivalence measured with an active microwave system. *J. Glaciol.*, 26(94), 225-233.

Fortin, R. 2000. *Caractérisation diélectrique du manteau neigeux à l'aide d'un radar UHF*, unpublished M.Sc. thesis, Université Laval, Québec, Canada.

Gubler, H. and M. Hiller. 1984. The use of microwave FMCW radar in snow and avalanche research. *Cold Reg. Sci. Technol.*, 9, 109-199.

Gubler, H. and P. Weilenmann. 1986. Seasonal snow cover monitoring using FMCW radar. *Proceedings of the International Snow Science Workshop* October 22-25, 1986, Lake Tahoe, ISSW Workshop Committee, Homewood, California, U.S.A. 87-97.

Herman, G. T., A. Lent and S. W. Rowland. 1973. ART: mathematics and applications. *J. theor. Biol.*, 42, 1-32.

Holmgren, J., M. Sturm, N. E. Yankielun and G. Koh. 1998. Extensive measurements of snow depth using FM-CW radar. *Cold Reg. Sci. Technol.*, 27, 17-30.

Marsh, P. 1999. Snowcover formation and melt: recent advances and future prospects. *Hydrol. Process.*, 13, 2117-2134.

Mätzler, C., 1996. Microwave permittivity of dry snow. *IEEE trans. Geosci. Remote Sensing*. 34(2), 573-581.

McMechan, G. A., 1983. Seismic tomography in boreholes. *Geophys. J. R. astr. Soc.*, 74, 601-612.

Niessen, J., E. Kliem, E. Pohkling and K.-P. Nick. 1994. The use of ground penetrating radar to search for persons buried by avalanches. *Proceedings of the 5th International Conference on Ground Penetrating Radar*, Kitchener, Ontario, Canada, 507-517.

Tiuri, M.E., A. Sihvola, E. G. Nyfors and M. T. Hallikainen. 1984. The complex dielectric constant of snow at microwave frequencies. *IEEE J. Ocean. Eng.*, OE-9(5), 377-382.

Vickers, R.S. and G.C. Rose. 1973. High resolution mesurements of snowpack stratigraphy using a short pulse radar. Proceedings of the eight International Symposium on Remote Sensing of Environment, 1972. vol 1. 261-277.

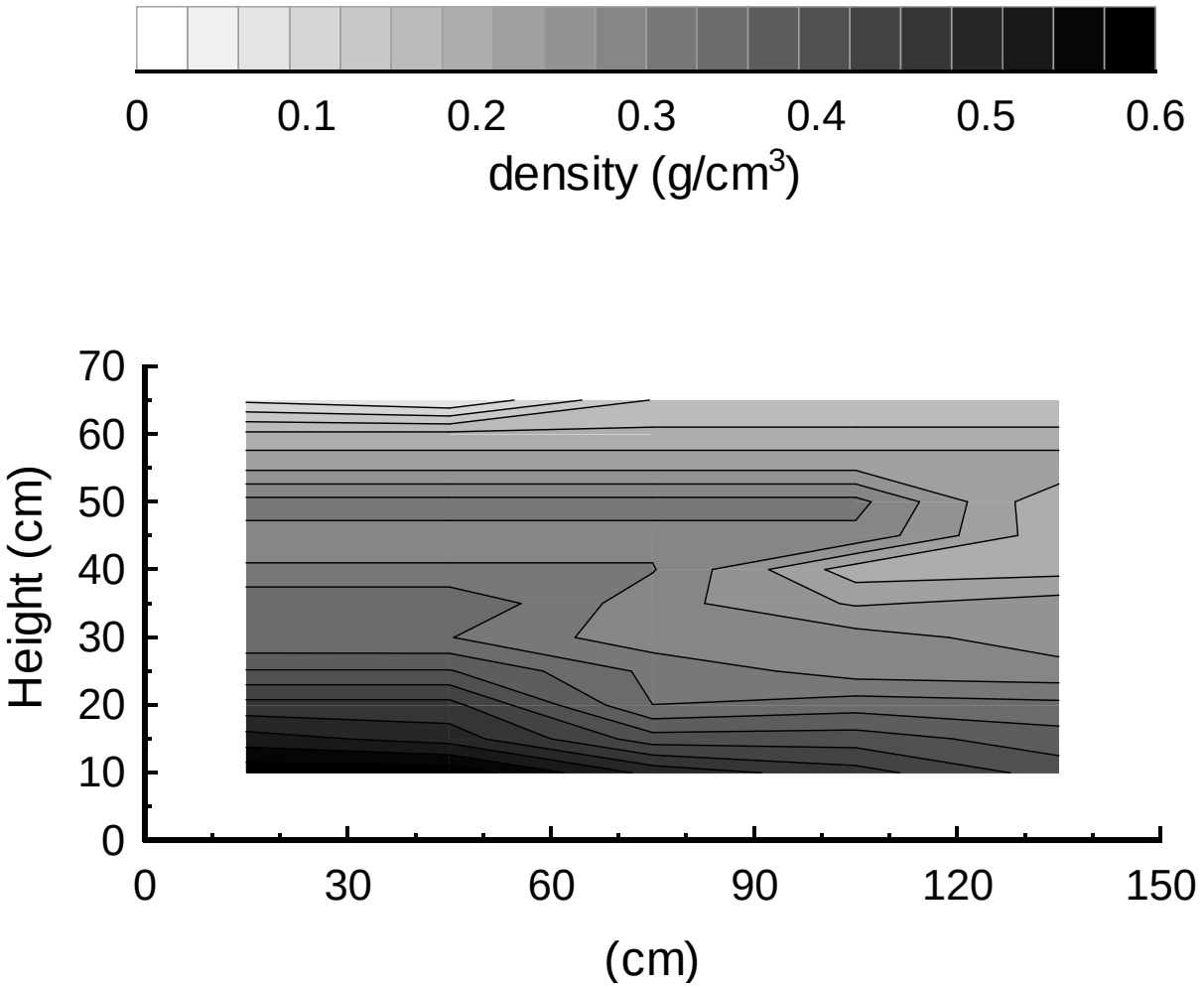

Figure 6. Tomographic image of the snowpack obtained with a bias-ART algorithm.